Turbulent phase screens generated by covariance approach and their application in numerical simulation of atmospheric propagation of laser beam

Hai-Xing Yan*, She Chen, and Shu-Shan Li
(Institute of Mechanics, Chinese Academy of Sciences, Beijing 100080, China)

ABSTRACT

Multiple phase screen (PS) method is typically used in numerical simulations of light propagation through a turbulent atmosphere and an adaptive optics (AO) system for phase compensation. One of key problems in it is generation of turbulent PS for describing the turbulent atmosphere. The covariance approach is a relatively new approach for generating PS. In this paper, the covariance approach is used to generate turbulent PS and a preliminary numerical simulation investigation on this approach and its generated PS is carried out. We propose to use three methods to evaluate the generated PS in a combining way. It is found that a comparison of the phase structure function of generated PS with the theoretical one is not enough and often inefficient. By contrast, a comparison of open loop and close loop laser propagation results by using generated PS can give a deeper insight. Open loop and close loop results by using PS generated by covariance approach are obtained and compared with those by using PS generated by spectral approach for the first time. It is shown that PS generated by covariance approach includes more abundant frequency components and these components have obvious influences on light propagation through a turbulent media.

Keywords: Atmospheric propagation of optical wave, Atmospheric turbulence, Phase screen, Multiple phase screen method, Covariance, Numerical simulation, Phase compensation

1. INTRUODUCTION

Generally, the multiple phase screen (PS) method is used to do numerical simulations of light propagation through a turbulent atmosphere and an adaptive optics (AO) system for phase compensation. PS are used to describe turbulent atmosphere. The structure constant of the index of refraction fluctuations, C_n^2, is used to characterize the turbulence strength.[1] The main idea of the multiple PS method is as following. The propagation path through the turbulent media can be divided into several segments which may have different lengths. It is thought that each segment may deform the phase of the optical wave independently. The contribution of the turbulent media segment to the phase distortion of the optical wave can be "pressed" into a very thin PS and added to the initial phase of the optical wave. It is assumed that the PS does not have a significant influence on the amplitude of the wave. The amplitude of the optical wave varies only in the propagation process of the wave with the deformed phase between two successive PS.

Obviously, generation of turbulent PS for describing the turbulent atmosphere is one of key problems in the multiple PS method. There are two main approaches for generating the PS. The first one is referred to as the spectral approach or FFT approach. The second one is referred to as the covariance approach. The latter is a relatively new

* Correspondence: Email: hxyan@imech.ac.cn; Phone: (86) 10 62554123; Fax: (86) 10 62561284.

XVI International Symposium on Gas Flow, Chemical Lasers, and High-Power Lasers, edited by Dieter Schuöcker,
Proceedings of SPIE Vol. 6346, 634628, (2007) 0277-786X/07/$18 doi: 10.1117/12.738905

approach for simulating the atmospheric turbulence. It is quite different from the conventional spectral approach. Although this approach has several specific advantages, its application in simulations of optical wave propagation through the turbulent atmosphere and an AO system has not been studied, and its comparison with the spectral approach is not analyzed in detail until now. The PS generator is numerically investigated in this paper. The computer program used for creating random arrays of phase values on grids of sampling points is compiled also.

2. PHASE SCREEN GENERATION APPORACH

Several approaches have been used to generate random PS with the proper point statistics and spatial and temporal correlation properties.[2] Conventional FFT based method or the spectral approach has been widely used to simulate atmospheric turbulence.[3, 4] In this approach, the low spatial frequency components cannot be properly represented in a simulation that is limited by the FFT algorithm. In order to properly account for the low frequency contribution to the PS, it is necessary to sample the spectrum at scales outside of the inertial range.[5-7] A totally different approach i.e. the covariance approach was proposed several years ago.[1, 2, 8-10] This approach does not have such low frequency limitation.

The Kolmogorov spectrum and the von Karman spectrum are commonly used in the atmospheric optics to describe a uniform isotropic turbulence. The Kolmogorov spectrum $\Phi_n^K(\kappa, z)$ is given by the following equation:

$$\Phi_n^K(\vec{\kappa}) = 0.033C_n^2\kappa^{-11/3} = 0.033C_n^2\left(\kappa_x^2+\kappa_y^2+\kappa_z^2\right)^{-11/6} \tag{1}$$

A simplified form of the von Karman spectrum that ignores the inner scale effect is given by:

$$\Phi_n^V = \frac{0.033C_n^2(z)}{(\kappa^2+4\pi^2/L_0^2)^{11/6}} \tag{2}$$

where L_0 is the outer scale of the atmospheric turbulence.

When using the delta function basis set, theoretical formulae for calculating the element of covariance matrix of the phase fluctuations for an *N*-Layer atmosphere are presented by Ref. [1], wherein Eq. (3.205) is for the von Karman spectrum and Eq. (3.214) is for the Kolmogorov spectrum.

Using the relationship of structure function and the correlation function

$$D_\psi(\vec{\rho}) = 2\left[\Gamma_\psi(0) - \Gamma_\psi(\vec{\rho})\right], \tag{3}$$

the phase structure function of von Karman power spectrum can be obtained:

$$\begin{aligned} D_\phi(\vec{\rho}) &= 2\times 3.089\times\sum_{i=1}^{N} r_{o_i}^{-5/3}\left[0.189\left(\frac{L_0}{\pi}\right)^{5/3} - \frac{(L_0/2\pi)^{5/6}K_{5/6}[2\pi\rho/L_0]\rho^{5/6}}{2^{5/6}\Gamma[11/6]}\right] \\ &= 6.178\times\sum_{i=1}^{N} r_{o_i}^{-5/3}\left[0.189\left(\frac{L_0}{\pi}\right)^{5/3} - \frac{(L_0/2\pi)^{5/6}K_{5/6}[2\pi\rho/L_0]\rho^{5/6}}{2^{5/6}\Gamma[11/6]}\right] \end{aligned} \tag{4}$$

where r_{o_i} is defined by

$$r_{0_i} = 0.185\left[4\pi^2/(k^2C_{n_i}^2\Delta z_i)\right]^{3/5} \tag{5}$$

For Kolmogorov power spectrum, the phase structure function is:

$$D_{\psi_i}(\rho) = 6.88\left(\rho/r_{o_i}\right)^{5/3}. \tag{6}$$

Direct simulation of PS can be achieved by using Singular Value Decomposition (SVD). Using SVD, the covariance matrix Γ_ϕ can be factorized into a product of three square matrix,[11] the eigenvalue diagonal matrix Λ of length *P* by *Q*, where *P* is the product of the grid point numbers in the *x* and *y* dimension and *Q* is the number of generated time-sequential PS. Λ is a matrix with eigenvalues on the diagonal and zero elsewhere, eigenvector column of U, and its transposed column of U^T where the superscript *T* represents the matrix transpose operator:

$$\Gamma_\phi = U\Lambda U^T \tag{7}$$

We generate a vector *b* of uncorrelated Gaussian random variables with zero mean and variance Λ.

$$E\left(bb^T\right) = \Lambda \tag{8}$$

Random PS are formed using:

$$a = Ub \tag{9}$$

This vector *a* is the column vector composed of the weights. Recall that when using the delta function basis set, the actual values of the weights correspond to the phase.

It is straightforward to verify this new vector *a* has a covariance of Γ_ϕ by using Eqs. (9) and (8):

$$E\left\{aa^T\right\} = E\left\{Ub\left(Ub\right)^T\right\} = E\left\{Ubb^TU^T\right\} = UE\left\{bb^T\right\}U^T = U\Lambda U^T = \Gamma_\phi \tag{10}$$

3. GENERATING AND EVALUAING PHASE SCREENS

In order to generate PS, the following steps can be carried out. First, based on Eq. (3.205) and Eq. (3.214) given by Ref. [1] and using widely available computation software packages,[11] the covariance matrix Γ_ϕ can be computed. Second, the covariance matrix corresponding to a specific power spectrum can be factorized by using special SVD algorithm. Third, a vector *b* of uncorrelated Gaussian random variables with zero mean and variance Λ can be obtained by using a proper random number generator. Finally, PS can be generated by the above-mentioned matrix operation. Here, FORTRAN has been used to accomplish such computation.

After obtaining the generated PS, evaluation of these screens is an important issue. Three different methods are proposed to evaluate the generated PS in a combining way in this paper.

Firstly, the accuracy of generated PS can be evaluated by means of a comparison of their phase structure function[1] over an appropriately sized ensemble with the theoretical phase structure function described in Eqs. (4) and (6). It is shown later that the agreement in this comparison is necessary for an appropriate PS, but this comparison is neither enough nor efficient. That is to say, in many cases different generated PS show an excellent agreement between their phase structure functions and the theoretical one, but quite different results and/or behaviors can be obtained from them.

The second method is directly to compare the covariance matrix $\Gamma_{\tilde{\phi}}$ of the generated PS with the theoretical covariance matrix Γ_ϕ. The $\Gamma_{\tilde{\phi}}$ can be calculated as follows

$$\Gamma_{\tilde{\phi}} = E\left[\tilde{\phi}\tilde{\phi}^T\right] \tag{11}$$

where $\tilde{\phi}$ is the vector of the generated random phases, $E\left[\bullet\right]$ is the ensemble average operator. The mean square error of all covariance array elements ε^2 can be computed, where ε^2 is given by:

$$\varepsilon^2 = \sum\left(\Gamma_\phi - \Gamma_{\tilde{\phi}}\right)^2 \Big/ (P\times Q)^2 \tag{12}$$

where the summation is taken over the whole covariance matrix.

The third method of evaluation is based on simulation computations of the optical wave propagation through the multiple generated PS (the open-loop results) and after having the phase compensation for its deformed wavefront (the close-loop results).[4] That is, open-loop and close-loop results by using the PS generated by the covariance approach can be compared with those by using the PS generated by the spectral approach. It is shown later that in this way the difference between two approaches can be compared and investigated more thoroughly and more deeply.

It is shown in this paper that in order to evaluate the generated PS more definitely, these three methods must be utilized in a combining way.

4. EXAMPLES OF GENERATED PHASE SCREENS AND DISCUSSION

In this section, some examples of PS generated by the covariance approach and by using the delta function basis set are shown. These random PS are separated in time. In order to compare with results of Ref. [1], the von Karman spectrum and the Kolmogorov spectrum are used to generate PS under the same conditions of Ref. [1]. There are 21 phase sampling points across one side of the aperture (i.e., P=21×21), which provided a sampling interval of $\Delta x=5\ cm$. Results for three temporal realizations of the PS (i.e., Q=3) are shown, which require computation and factorization of 1323×1323 element covariance arrays.

Figure 1 shows the surface plots and grey scale images of three time-sequential PS created by the covariance approach for the von Karman spectrum. The grey scale images were created by linearly stretching the phase values between 0 and 255 gray levels. For briefness, PS for the Kolmogorov spectrum are not presented here. All these PS results are very well comparable to those of Ref. [1].

The average phase structure function of PS generated by the covariance approach for the von Karman spectrum have been calculated and shown in Fig. 2. Phase structure functions of PS generated by the spectral approach for the von Karman spectrum under the same conditions without and with low frequency correction are shown in Fig. 2 also. In comparison to the theoretical phase structure function, result of the covariance approach is the best; the difference between it and the theoretical one is negligible. The average phase structure function of PS generated by the spectral approach without low frequency correction shows a quite large difference in the low space frequency region in comparison to the theoretical one; after including the low frequency correction, the comparison of results of the spectral approach with the theoretical one gets better as the low frequency correction of higher order is included; but the agreement is not as perfect as that of the covariance approach results. In fact, the phase structure function of PS generated by the covariance approach for the Kolmogorov spectrum is calculated as well and similarly, it can compare with the theoretical one for the Kolmogorov spectrum very well. For briefness, these results are not included here.

The wind velocities in Fig. 1 are chosen as $v_x=0\ m/s$ and $v_y=10\ m/s$, where v_x and v_y are the x- and y-directed component of $\vec{v}(z)$, respectively. From seeing Fig. 1, it is very easy to find the movement of the major structure in PS is only in the y-direction. Because the time interval between two sequential PS is set to be 0.01s, the movement of the major structure is exactly two sampling intervals of 10 cm in the y direction. From the grey scale plot, the movement is along the downward direction (corresponding to the y increasing direction). By carefully comparing the sequential grey scale images and data in the corresponding column of the sequential phase screens, it can be found that there is certain surface deformation in the PS in addition to the major structure's movement.

On the other hand, effects of the lateral wind and the Taylor's frozen field hypothesis in the spectral approach are expressed in the following way: to produce large enough PS by using the spectral approach; to choose certain areas among them as the initial areas corresponding to the optical path of beacon; because of the lateral wind and the time

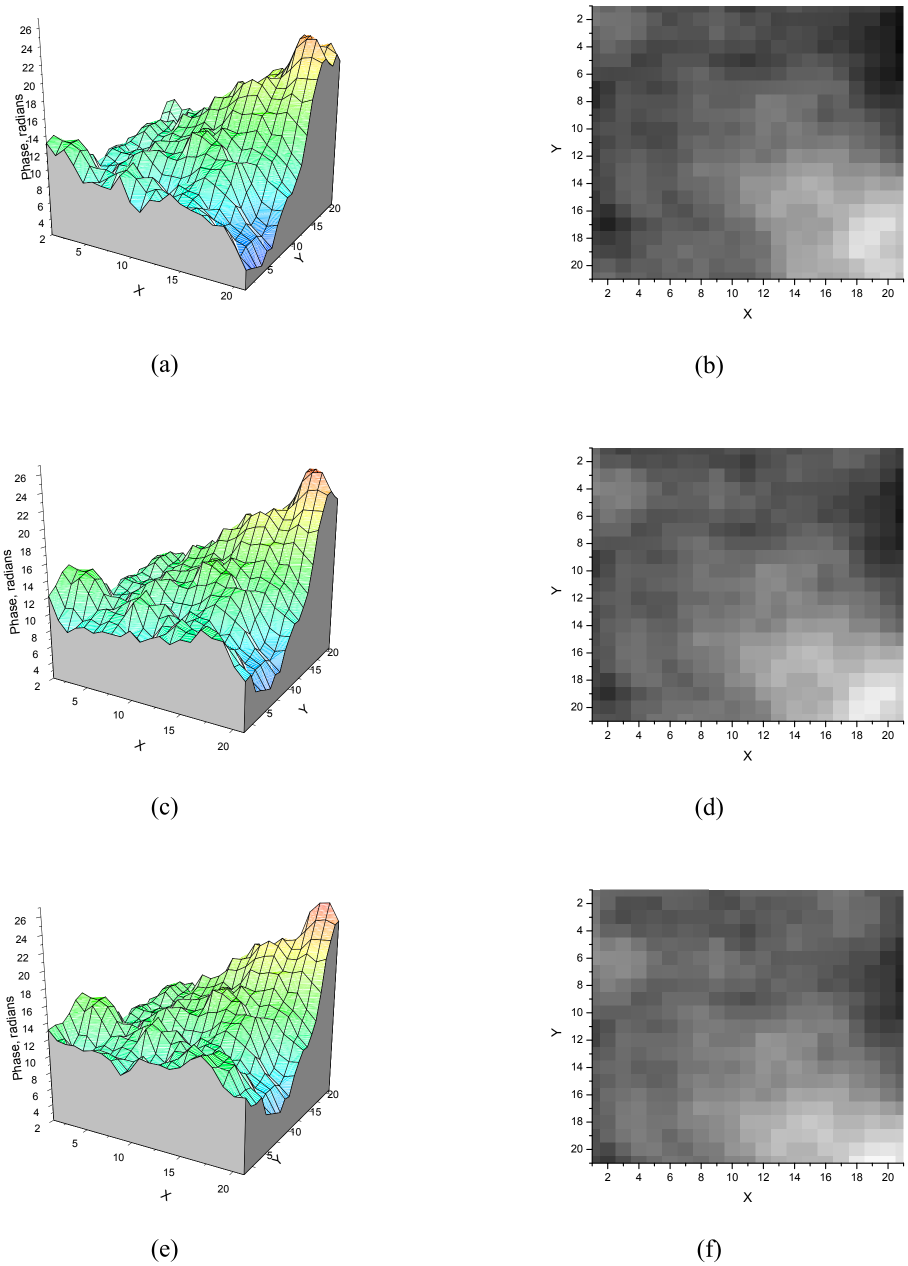

Fig. 1 Three random, time-sequential PS images for the case of atmospheric layers moving in the same direction and speed, and for the von Karman spectrum: (a) surface plot of PS, *t=0 s*; (b) grey scale image of (a); (c) surface plot of PS, *t=0.01 s*; (d) grey scale image of (c); (e) surface plot of PS, *t=0.02 s*; (f) grey scale image of (e).

delay, PS move certain distance(s) within the time delay along the wind direction which is perpendicular to the light propagation direction. Because the large PS remain to be not varied in the whole process, there is no surface deformation for the PS generated by the spectral approach at all.

Like this, an important question appears: based on the same Taylor's frozen field hypothesis, movement of major structure and surface deformation exist in PS generated by the covariance approach, however, there is no surface deformation in addition to the movement of major structure in PS generated by the spectral approach; which approach is better for generating PS?

Taylor's frozen field hypothesis is utilized in the spectral approach after the generation of the PS. This is why the PS only move along the wind direction, and have no deformation at all. On the other hand, in the covariance approach the frozen field hypothesis is introduced in the process of calculating the covariance matrix, and the effect of such hypothesis has been "naturally" included in the generated PS. By investigating the algorithm, it is found that the number of singular values in the eigenvalue diagonal matrix is more than the product P of the grid point numbers in the x and y dimension of PS. Generally, a singular value corresponds to space frequency component(s). More none-zero singular value appeared in the eigenvalue diagonal matrix means that more space frequency components are included in the PS generated by the covariance approach. We imagine that the influence of these more abundant frequency components is to produce the PS surface deformation. In fact, the real atmospheric turbulence should be much more complicated than the Taylor's frozen field hypothesis. At sequential moments, in addition to the effect of the lateral wind, real-time deformations exist in the atmospheric turbulence and frequency components in the practical atmosphere should be much more abundant than that the limited density of PS can reflect. The time-sequential PS generated by the covariance approach are generated as a whole simultaneously. Thus, these PS should include more information than those PS generated by the spectral approach do. The latter can only express the major structure shift. From this point of view, the PS generated by the covariance approach should be more realistic than those generated by the spectral approach.

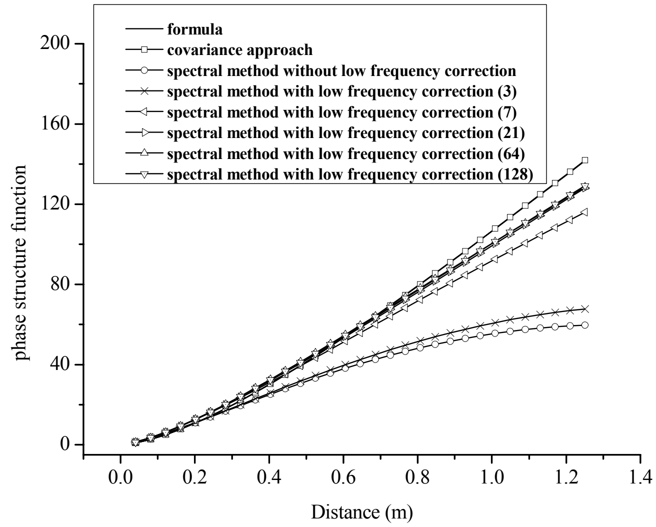

Fig. 2 Comparison of phase structure functions (I)

In order to investigate the effect of different space frequency components, under the condition that the singular value number is greater than the number of sampling points, we artificially delete some singular values having smaller amount from the eigenvalue diagonal matrix. This is equivalent to removing the effect of some more abundant space frequency components in the covariance approach. After such artificial treatment, the movement of major structure remains in the generated PS, but the surface deformation of PS disappears. That is to say, the PS generated after this treatment are equivalent to those generated by the spectral approach. In fact, when carefully checking and comparing data in the time-sequential PS, it can be found that phase data in each previous PS after shifting two sampling intervals in the y direction are exactly same to those in the successive PS after removing "extra" singular values. It is shown that more abundant frequency components exist in the PS generated by the covariance approach and these components produce the surface deformation in the PS.

For checking the influence of this treatment on the phase structure function of the generated PS, 100,000 times average phase structure functions before and after removing smaller singular values are calculated and compared with the theoretical one. Fig. 3 shows the corresponding result. Fig. 3 shows that this treatment does not have obvious influence on the phase structure function, the phase structure functions before and after the treatment are very well comparable to the theoretical one. It means that the effluence of more abundant space frequency components cannot be reflected in the phase structure function. It is also shown that it is not enough only to compare the phase structure function of the generated PS with the theoretical one for evaluating quality of the generated PS.

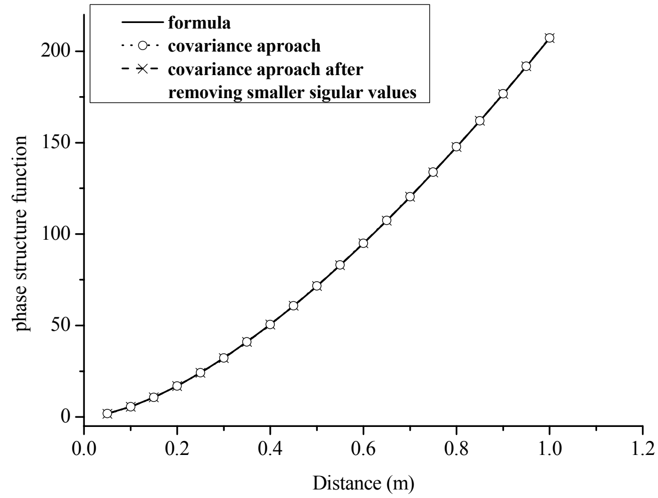

Fig. 3 Comparison of phase structure functions (II)

5. RESULTS OF LIGHT PROPAGATION AND PHASE COMPENSATION AND DISCUSSION

In this section, simulation computational results of atmospheric propagation of an optical wave and its phase compensation by using the random PS generated by the covariance approach and by the spectral approach are presented and compared. This is one of the important methods to evaluate the covariance approach in our point of view.

Six scenes are chosen as the light propagation scenes. Similar to our previous work,[4] long-exposure results of atmospheric propagation without and with static phase compensation having time delay are calculated using 3000 sets of random PS generated by the two approaches. PS generated by the spectral approach without and with low frequency correction are used to do the simulation computation separately. Results for the von Karman (VON) spectrum and the Kolmogorov (KOL) spectrum are calculated separately, using Strehl ratios, STRC and STRCC,[4] as the evaluation parameters. The main computational conditions are as follows: 3 km horizontal propagation path is chosen; the whole propagation path is evenly separated into 10 segments; a focusing light beam is adopted; a constant lateral wind speed along *x* direction is used for 10 PS, the wind speed of y direction is chosen as 0; C_n^2 is assumed to be uniform along the optical path; the grid number of calculation is 32×32; the delay time is 2.75ms; the light wavelength is 632.8nm; the aperture size is 60 cm.

Because of the limitation of computer capability, a larger grid number cannot be used and it is impossible to carry out a simulation of a practical AO system including dynamic control process under the present condition. This is why the complete phase compensation[4] is used in this paper. The complete phase compensation means that after a light beam passes through the turbulent atmosphere (i.e. the turbulent PS) the distorted wavefront can be obtained at the incoming aperture and a minus sign (-) is taken for all the grid point of the distorted wavefront in the emission aperture. Finally, the phase compensated beam (the light beam having minus distorted wavefront) propagates in the opposite direction and through a translated (because of the time delay and the lateral wind) turbulent media again to reach the target. The complete phase compensation is much simpler than a practical AO system, but it represents a specific kind of the phase compensation for the distorted wavefront. Open loop results without phase compensation and close loop results with phase compensation are calculated. For briefness, results of only three scenes are shown in Table 1.

Table 1 Comparison of simulation results of atmospheric propagation and phase compensation using PS generated by the covariance approach and by the spectral approach (I)

Computational condition		Open loop		Close loop	
		STRC	STRCC	STRC	STRCC
Wind velocity *2.22m/s* r_0=*9.504cm*	Spectral approach without low frequency correction	0.1037	0.3743	0.8720	0.8909
	Spectral approach with low frequency correction	0.09181	0.3336	0.8753	0.8935
	Covariance approach for VON	0.02465	0.1035	0.9206	0.9467
	Covariance approach for KOL	0.01885	0.07922	0.9299	0.9502
Wind velocity 2.42*m/s* r_0=*3.051cm*	Spectral approach without low frequency correction	0.01822	0.07701	0.6362	0.6984
	Spectral approach with low frequency correction	0.01676	0.06995	0.6340	0.6967
	Covariance approach for VON	0.008950	0.03875	0.5522	0.6775
	Covariance approach for KOL	0.008999	0.03897	0.5837	0.6853
Wind velocity 3.14*m/s* r_0=*1.716cm*	Spectral approach without low frequency correction	0.009365	0.04092	0.3003	0.4408
	Spectral approach with low frequency correction	0.009448	0.04041	0.2941	0.4366
	Covariance approach for VON	0.009216	0.03983	0.08877	0.2356
	Covariance approach for KOL	0.009244	0.03988	0.1042	0.2663

It is shown in Table 1 that difference between open loop results of two approaches is relatively apparent in the case of weaker turbulence. As the turbulence intensity gets stronger, the difference becomes smaller. In the case of strong turbulence, results of the covariance approach can be well compared with those of the spectral approach. In contrast, close loop results of two approaches can be well compared in case of weaker turbulence; as the turbulence gets stronger, close loop results of the covariance approach is obviously lower than those of the spectral approach. In addition, change of open loop results of the spectral approach after including the low frequency correction is noticeable but not very large in the case of weaker turbulence; it is negligible in the case of stronger turbulence; and change of close loop results of the spectral approach after including the low frequency correction is negligible in the case of either weaker turbulence or stronger turbulence. Further, difference of the covariance approach results using two different power spectrums, i.e. von Karman spectrum and Kolmogorov spectrum is quite small.

Table 2 Comparison of simulation results of atmospheric propagation and phase compensation using PS generated by the covariance approach and by the spectral approach (II)

Computational condition		Open loop		Close loop	
		STRC	STRCC	STRC	STRCC
Wind velocity *2.22m/s* R_0=*9.504cm*	Covariance method – original	0.02465	0.1035	0.9206	0.9467
	Covariance method – smaller eigenvalues removed	0.02623	0.1074	0.9394	0.9657
Wind velocity 2.42*m/s* R_0=*3.051cm*	Covariance method – original	0.008950	0.03875	0.5522	0.6775
	Covariance method – smaller eigenvalues removed	0.009062	0.03925	0.6416	0.7882
Wind velocity 3.14*m/s* R_0=*1.716cm*	Covariance method – original	0.009216	0.03983	0.08877	0.2356
	Covariance method – smaller eigenvalues removed	0.008942	0.03963	0.1823	0.3888

Open loop results and close loop results by using PS generated by the covariance approach for von Karman spectrum after removing "extra" smaller singular values are calculated and shown in Table 2. It can be found that after removing "extra" smaller singular values artificially, the open loop results do not show great changes and the close loop results of the covariance approach tend to those of the spectral approach, although there still exist some obvious differences between them. This tendency is consistent with our expectation. After removing the frequency components corresponding to smaller singular values, the correlation of successive PS has been improved and the phase surface deformation has been removed. This is why the close loop results of the covariance approach tend to those of the spectral approach and this tendency is more obvious for stronger turbulence. On the other hand, existence of some obvious difference between the covariance approach results and the spectral approach results indicates that the PS generated by the covariance approach are still not equivalent to those generated by the spectral approach even after removing "extra" smaller singular values artificially in the covariance approach.

Following the similar thought, for further investigating the covariance approach, four largest singular values and other "extra" smaller singular values are removed from the eigenvalue matrix simultaneously. Then, open loop results and close loop results by using PS generated by the covariance approach for the von Karman spectrum are calculated and shown in Table 3. It can be found that after removing four largest singular values and other "extra" smaller singular values artificially, the open loop results of the covariance approach show larger changes in the case of weaker turbulence and tend to those of the spectral approach; however, the open loop results of the covariance approach do not show obvious change in the case of stronger turbulence; meanwhile, the close loop results of the covariance approach show some increases and tend to those of the spectral approach. After comparing to Table 2, it is found that these increases of the close loop results basically come from the treatment removing smaller singular values. The treatment removing four largest singular values does not have obvious influence on the close loop results (see Table 3).

Table 3 Comparison of simulation results of atmospheric propagation and phase compensation using PS generated by the covariance approach and by the spectral approach (III)

Computational condition		Open loop		Close loop	
		STRC	STRCC	STRC	STRCC
Wind velocity *2.22m/s* R_0=*9.504cm*	Covariance method – original	0.02465	0.1035	0.9206	0.9467
	Covariance method – 4 largest and other "extra" smaller eigenvalues removed	0.06574	0.2408	0.9433	0.9659
Wind velocity 2.42*m/s* R_0=*3.051cm*	Covariance method – original	0.008950	0.03875	0.5522	0.6775
	Covariance method – 4 largest and other "extra" smaller eigenvalues removed	0.01077	0.04580	0.6633	0.7906
Wind velocity 3.14*m/s* R_0=*1.716cm*	Covariance method – original	0.009216	0.03983	0.08877	0.2356
	Covariance method – 4 largest and other "extra" smaller eigenvalues removed	0.009445	0.03990	0.1622	0.3886

6. CONCLUSION

The covariance approach using delta function as base function is used to generate PS for the von Karman spectrum and for the Kolmogorov spectrum and a preliminary numerical simulation investigation is carried out. The generated PS under the same conditions can be very well compared with those in Ref. [1]. Phase structure functions of PS generated by the covariance approach agree excellently with the theoretical one. We propose to use three methods to evaluate the generated PS in a combining way. It is found that a comparison of the phase structure function of generated PS with the theoretical one is not enough and often inefficient. By contrast, a comparison of open loop and close loop laser propagation results by using generated PS can give a deeper insight. When the successive PS with temporal correlation property are generated, phase surface deformations have been found in addition to the movement of major structure. It is shown that these surface deformations can be removed by deleting the "extra" smaller singular values in the covariance matrix and at the same time the phase structure function of generated PS does not have an obvious change. Open loop results and close loop results by using PS generated by the covariance approach are obtained and compared with those by using PS generated by the spectral approach for the first time within our knowledge. It is found that the open loop results of the covariance approach are lower than those of the spectral approach in case of weaker turbulence and its close loop results are obviously lower than those of the spectral approach in case of stronger turbulence. After deleting the "extra" smaller singular values, the close loop results of the covariance approach tend to those of the spectral approach, and there is no obvious effect on the open loop results. If deleting four largest singular values at the same time, the open loop results of the covariance approach tend to those of the spectral approach also. These indicate that the PS generated by the covariance approach include more abundant frequency components than those generated by the spectral approach and these frequency components have obvious influences on the open loop results and the close loop results.

This paper presents a preliminary numerical investigation of the covariance approach. There are a lot of important problems left for further work.

REFERENCE

1. M. C. Roggemann, B. M. Welsh, “Imaging through Atmospheres,” CRC Press, 1996
2. T. Goldring, L. Carlson, “Analysis and implementation of non-Kolmogorov phase screens appropriate to structured environments,” Proc. SPIE, vol.1060 243-264, 1989
3. J. A. Fleck, Jr., J. R. Morris, M. D. Feit, “Time-dependent propagation of high energy laser beams through the atmosphere,” Appl. Phys., vol. 10, 129-160, 1976
4. Hai-Xing Yan, Shu-Shan Li, De-Liang Zhang, She Chen “Numerical simulation of an adaptive optics system with laser propagation in the atmosphere,” Appl. Opt., vol. 39, 3023-3031, 2000
5. J. M. Martin, S. M. Flatté, “Intensity images and statistics from numerical simulation of wave propagation in 3-D random media,” Appl. Opt., vol. 27, 2111-2126, 1988
6. R. Flehlich, “Simulation of laser propagation in turbulent atmosphere,” J. Opt. Soc. Am. A, vol. 39, 393-397, 2000
7. B.J. Herman, L.A. Strugala, “Method for inclusion of low-frequency contributions in numerical representation of atmospheric turbulence,” Proc. SPIE. vol. 1221, 183-192, 1990
8. A.D. McAulay, “Artificial turbulence generation alternatives for use in computer and laboratory experiments,” Proc. SPIE, Vol. 4493, 141-149, 2001
9. A. D. McAulay, “Generating Kolmogorov phase screens for modeling optical turbulence,” Proc. SPIE, Vol. 4034, 50-57, 2000
10. C.M. Harding, R.A. Johnston, R.G. Lane, “Fast simulation of a Kolmogorov phase screen,” Applied Optics Vol. 38, 2161-2170, 1999
11. “Math library/Special function,” in IMSL FORTRAN Subroutines for mathematical Applications, 1998
12. J. W. Goodman, “Statistical Optics,” New York: John Wiley & Sons, 1985
13. W. H. Press, B. P. Flannery, S. A. Teukolsky, W. T. Vetterling, “Numerical Recipes –The Art of Scientific Computing,” Cambridge, UK: Cambridge University Press, 2 Edition, 1992)